iScience

CellPress
OPEN ACCESS

Article

Anti-viral efficacy of a next-generation CD4-binding site bNAb in SHIV-infected animals in the absence of anti-drug antibody responses

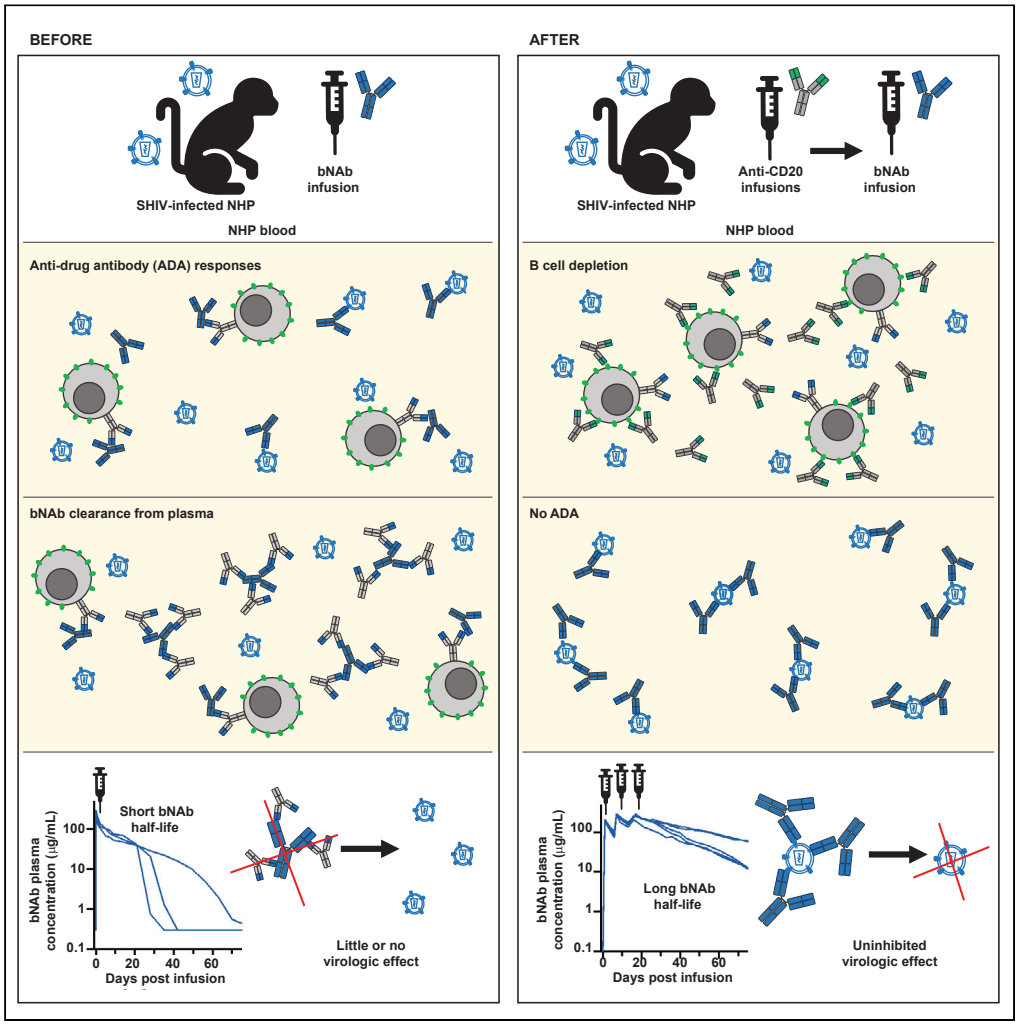

Sarah E. Lovelace, Sabrina Helmold Hait, Eun Sung Yang, ..., Richard A. Koup, John R. Mascola, Amarendra Pegu

pegua@niaid.nih.gov

Highlights

Highly potent CD4bs bNAb reduces viremia up to 4 log_{10} in SHIV-infected animals

Sustained B cell depletion prevents development of ADA responses

Lack of ADA enables multiple bNAb infusions over 12 weeks

Lovelace et al., iScience 25, 105067
October 21, 2022
https://doi.org/10.1016/j.isci.2022.105067

iScience

CellPress
OPEN ACCESS

Article

Anti-viral efficacy of a next-generation CD4-binding site bNAb in SHIV-infected animals in the absence of anti-drug antibody responses

Sarah E. Lovelace,[1] Sabrina Helmold Hait,[1] Eun Sung Yang,[1] Madison L. Fox,[1] Cuiping Liu,[1] Misook Choe,[1] Xuejun Chen,[1] Elizabeth McCarthy,[1] John-Paul Todd,[1] Ruth A. Woodward,[1] Richard A. Koup,[1] John R. Mascola,[1] and Amarendra Pegu[1,2,*]

SUMMARY

Broadly neutralizing antibodies (bNAbs) against HIV-1 are promising immunotherapeutic agents for treatment of HIV-1 infection. bNAbs can be administered to SHIV-infected rhesus macaques to assess their anti-viral efficacy; however, their delivery into macaques often leads to rapid formation of anti-drug antibody (ADA) responses limiting such assessment. Here, we depleted B cells in five SHIV-infected rhesus macaques by pretreatment with a depleting anti-CD20 antibody prior to bNAb infusions to reduce ADA. Peripheral B cells were depleted following anti-CD20 infusions and remained depleted for at least 9 weeks after the 1st anti-CD20 infusion. Plasma viremia dropped by more than 100-fold in viremic animals after the initial bNAb treatment. No significant humoral ADA responses were detected for as long as B cells remained depleted. Our results indicate that transient B cell depletion successfully inhibited emergence of ADA and improved the assessment of anti-viral efficacy of a bNAb in a SHIV-infected rhesus macaque model.

INTRODUCTION

Broadly neutralizing antibodies (bNAbs) against HIV-1 target conserved regions on the HIV-1 envelope glycoprotein (Env) and mediate potent neutralization of a broad range of circulating HIV-1 strains (Griffith and McCoy, 2021; Sok and Burton, 2018; Walsh and Seaman, 2021). Due to their intrinsic antibody properties, bNAbs possess relatively long half-lives in the range of 2–4 weeks and mediate multiple effector functions through Fc receptors (Cohen et al., 2019; Gaudinski et al., 2018, 2019; Mayer et al., 2017). Many of these bNAbs have now progressed to clinical testing for both prevention and treatment of HIV-1 infection (Bar-On et al., 2018; Corey et al., 2021; Crowell et al., 2019; Edupuganti et al., 2021; Mahomed et al., 2020; McFarland et al., 2021; Mendoza et al., 2018; Stephenson et al., 2021). These initial clinical studies have shown potent antiviral activity of these bNAbs and demonstrate the potential for their use in the treatment of HIV-1 infection. These results also suggest that use of a combination of bNAbs or multispecific antibodies may be required for long-term viral suppression to prevent viral escape. In addition, through further antibody isolation and engineering, more potent bNAbs have been reported providing a next generation of bNAbs that can be clinically tested (Kwon et al., 2021; Pegu et al., 2022; Schommers et al., 2020). Due to high cost of conducting human studies, these bNAbs are tested in preclinical models for their antiviral efficacy before being advanced into clinical development.

The nonhuman primate model is a widely used model for evaluation of therapeutics against HIV-1. In this model, rhesus macaques are infected with a chimeric simian-human immunodeficiency virus (SHIV) that expresses HIV-1 Env in the backbone of simian immunodeficiency virus (SIV) structural genes (Bauer and Bar, 2020). bNAbs have been administered to SHIV-infected rhesus macaques to demonstrate their anti-viral efficacy (Barouch et al., 2013; Julg et al., 2017; Nishimura et al., 2021; Shapiro et al., 2020; Shingai et al., 2013; Spencer et al., 2022; Wen et al., 2021). These studies have shown potent anti-viral activity after either single or multiple infusions of bNAbs. However, a limitation of these studies has been the rapid development of xenogeneic anti-drug antibody responses (ADA) against the bNAb itself in many cases (Lee et al., 2021). This ADA response greatly affects the pharmacokinetic profile of bNAbs by rapidly clearing them from circulation and compromising the assessment of bNAb anti-viral efficacy in these studies. In addition,

[1]Vaccine Research Center, National Institute of Allergy and Infectious Diseases (NIAID), National Institutes of Health (NIH), Bethesda, MD 20892, USA

[2]Lead contact

*Correspondence: pegua@niaid.nih.gov

https://doi.org/10.1016/j.isci.2022.105067

this ADA response hampers the ability of testing prolonged treatment with bNAbs via multiple infusions, further limiting the ability to assess long-term efficacy of bNAb treatments on viral evolution and escape.

Rituximab is one of the first antibody drugs that was licensed for treatment of B cell malignancies and leads to a rapid depletion of B cells from circulation (Klein et al., 2021; Maloney et al., 1997; Marshall et al., 2017; McLaughlin et al., 1998). It targets the CD20 surface antigen on B cells and is a recombinant chimeric murine/human type I anti-CD20 monoclonal antibody. It has been used previously in rhesus macaques to deplete $CD20^+$ B cells for studying the effect of humoral responses on infection (Carroll et al., 2011; Gaufin et al., 2009; Miller et al., 2007; Permar et al., 2004; Schmitz et al., 2003; Tasca et al., 2011), suppressing rejection of corneal transplants (Choi et al., 2018; Kim et al., 2018; Yoon et al., 2020), and reducing B cell tumors (Qin et al., 2019). For assessing the role of humoral responses in infection, $CD20^+$ B cells were depleted prior to viral challenge or immunization with the antigen of interest. These studies saw stunted or delayed humoral responses to viral challenge or vaccination. Similarly, in studies of corneal xenotransplantation, $CD20^+$ B cell depletion on its own and in combination with other immunosuppressants given at the time of transplant can extend survival of the graft and prevent rejection. These studies suggest that B cell depletion using an anti-CD20 antibody can effectively reduce formation of *de novo* humoral responses. Here, we depleted $CD20^+$ B cells in 5 SHIV-infected rhesus macaques using a rituximab-based afucosylated rhesusized anti-CD20 antibody to assess whether temporary B cell depletion prior to bNAb administration might reduce or eliminate ADA and improve the assessment of the anti-viral efficacy of a bNAb.

RESULTS

In vivo B cell depletion after anti-CD20 infusion

We assessed whether depletion of B cells in nonhuman primates (NHPs) prior to infusion with a bNAb could reduce the anti-drug response which often forms following bNAb infusion. For this purpose, we used rhesus macaques (n = 5) that were chronically infected with $SHIV_{BG505}$ for a period of 1–4 years. These viremic animals were then treated with a rhesusized version of a rituximab-based anti-CD20 antibody which had been afucosylated to enhance antibody-dependent cellular cytotoxicity. Three 50 mg/kg infusions of the afucosylated rhesusized anti-CD20 (anti-CD20) were given intravenously (IV) two weeks apart; that was followed with three weekly infusions of a bNAb (Figure 1A). As soon as 2 days following the first anti-CD20 infusion, B cells were no longer detectable in whole blood staining for CD20 by flow cytometry (Figure 1B). This early loss of CD20 expression was observed in all 5 animals. The depleting anti-CD20 Ab was shown to compete for binding with the anti-CD20 Ab used for flow cytometric analysis (Figure S1A), therefore B cell depletion was verified by flow cytometry of PBMCs collected weekly throughout the study and stained for expression of B cell marker CD19 (Figure S1B). A distinct B cell population reappeared in the whole blood staining of each animal as soon as 8 weeks or as late as 18 weeks following the last anti-CD20 infusion (Figure 1C). NHPs 3 and 5 saw a complete return of B cell counts to the baseline levels, NHP 1 had cell counts level off at a new baseline lower than the original, and NHPs 2 and 4 had cell counts below baseline but still increasing by the time sample collection was stopped. After anti-CD20 infusion, plasma concentration of this Ab increased sharply but was quickly cleared from the plasma with a half-life of 3.9 days (Figure 1D). Autologous anti-Env antibody binding titers appeared to drop throughout B cell depletion but began to increase later generally coinciding with onset of B cell return (Figure S2B). This drop in SHIV-specific humoral response, while not insignificant, did not appear to affect viremia with minimal changes observed during this initial period of B cell depletion (Figure 2A). The total IgG levels in these animals fluctuated over time and showed a slight decrease in some animals following B cell depletion (Figure S2A). Animals that experienced a drop in total IgG levels showed a return to baseline values corresponding with their recovery of B cells.

Potent viral suppression after multiple infusions of VRC01v23

After depletion of B cells by anti-CD20 infusion, we administered the bNAb VRC01v23, a CD4-binding site-specific bNAb variant derived from VRC01.23 with improved breadth and potency over VRC01 (Kwon et al., 2021). Plasma viral loads dropped significantly in all viremic animals after the first treatment with VRC01v23, as much as 2.5 and 3 $\log_{10}$ reductions of viral copies per milliliter of blood in animals with the highest viral loads, NHPs 1 and 3, respectively (Figure 2A). 3 out of 4 viremic animals had viral loads reduced to below the limit of detection after the 1^{st} or 2^{nd} infusion, while the 4^{th} animal (NHP 3) experienced a substantial reduction of up to 3.7 $\log_{10}$ but still maintained low levels of viremia after all 3 infusions. The plasma concentration of VRC01v23 showed an increase after each 10 mg/kg infusion, reaching up to 300 μg of bNAb per milliliter of blood (μg/mL) when measured within 1–3 days following each infusion. (Figure 2B). VRC01v23 had a half-life of between 12.1 and 27.6 days following the final infusion of the dosing regimen

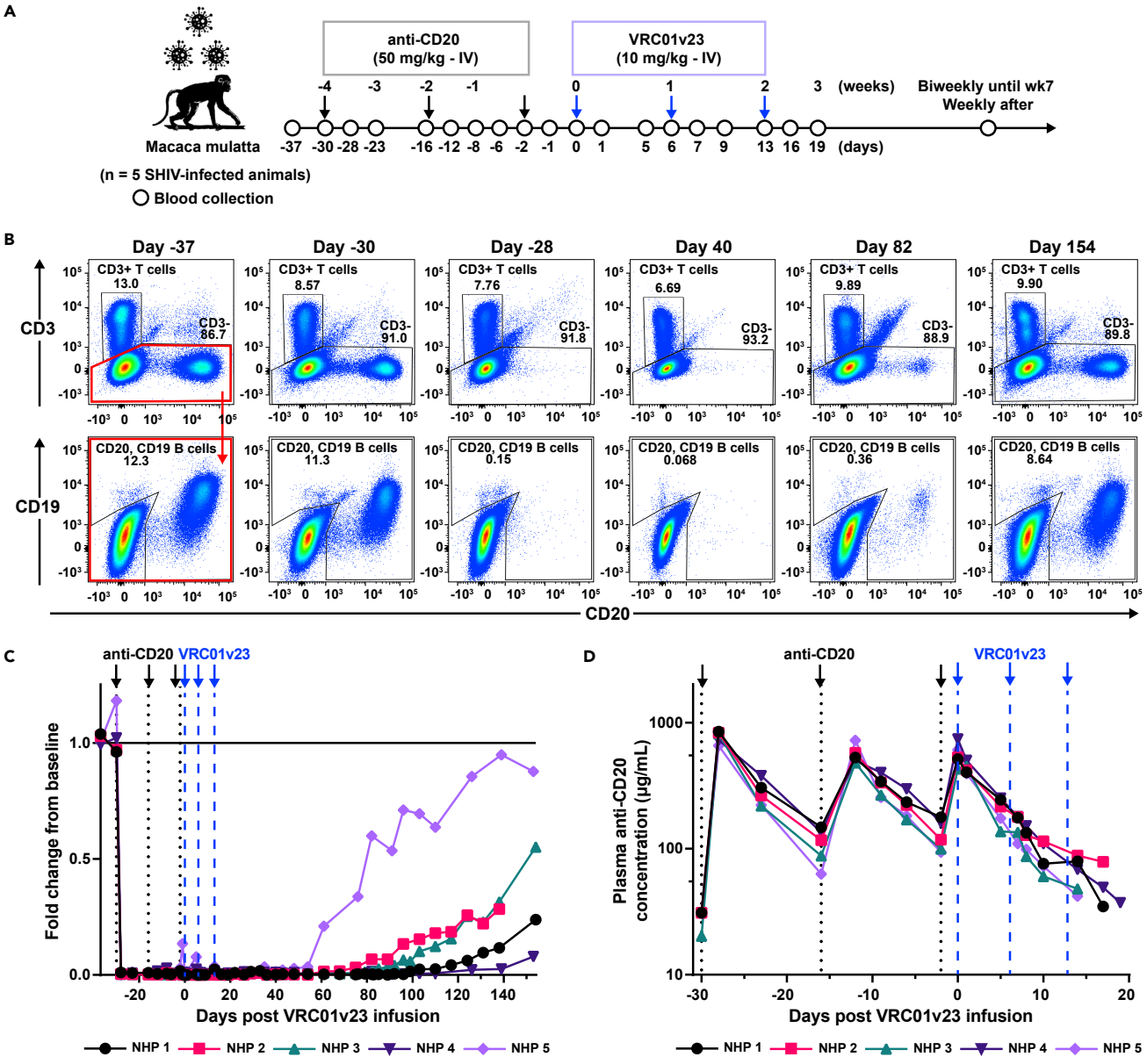

Figure 1. Study design and *in vivo* B cell depletion after anti-CD20 infusion

(A) SHIV-infected rhesus macaques were treated with intravenous (IV) infusions of 50 mg/kg afucosylated rhesusized anti-CD20 (anti-CD20, black arrows) followed by 10 mg/kg of bNAb VRC01v23 (blue arrows). Blood was sampled at indicated timepoints over the course of the study.

(B) Representative flow cytometry plots of whole blood $CD20^+$ B cells and total $CD3^+$ T cells at days -37, -30, -28, 40, 82, and 154 of VRC01v23 infusion in NHP 3. B cell counts determined by number of $CD19^+$ and/or $CD20^+$ events after gating on $CD3^-$ leukocytes. Peripheral B cell depletion was already seen 2 days following first anti-CD20 infusion.

(C) $CD19^+$ and/or $CD20^+$ B cell counts in whole blood obtained by flow cytometry for each macaque normalized to its $CD19^+$ and/or $CD20^+$ B cell count average from day –37 and day 30 of bNAb infusion, prior to CD20 depletion (black arrows/dotted lines = anti-CD20 infusions, blue arrows/dashed lines = VRC01v23 infusions).

(D) Pharmacokinetics (PK) of anti-CD20 in macaque plasma following three 50 mg/kg IV infusions (LOD = 31 µg/mL). See also Figures S1 and S2.

(Table 1). The rate at which viral loads rebounded following VRC01v23 infusion varied and did not seem to correlate with plasma concentration of the bNAb (Figure 2B). NHP 3 rebounded within 3 weeks following the last infusion of the bNAb with plasma concentrations as high as 227 µg/mL (2B, top right). Two more animals, NHPs 1 and 5, rebounded within 4 weeks following the last bNAb infusion, with bNAb concentrations of 89 and 189 µg/mL, respectively (2B, bottom right, top left). NHP 2 maintained viral suppression

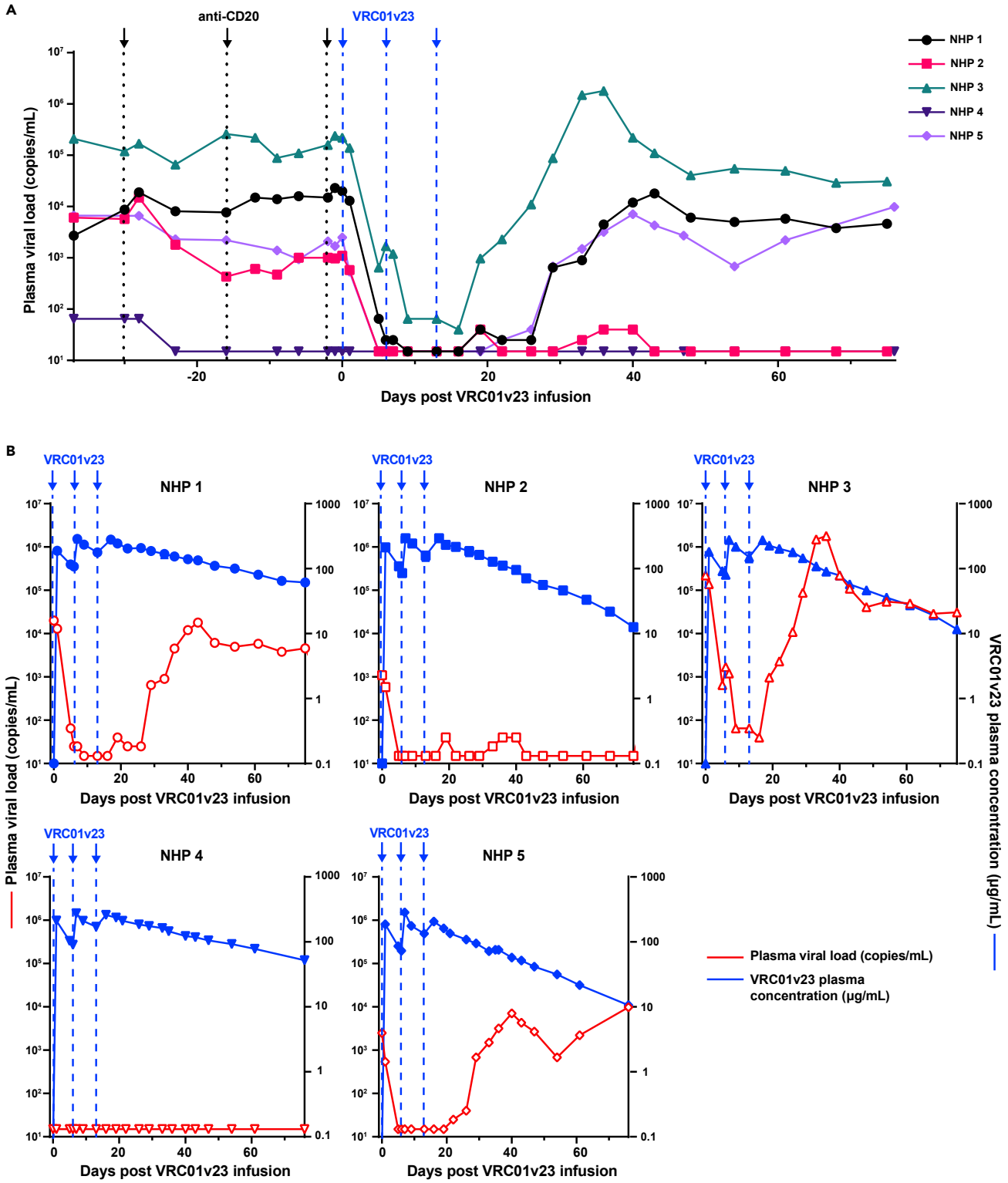

Figure 2. VRC01v23 anti-viral efficacy and pharmacokinetics

(A) Plasma viral load (LOD = 15 copies/mL) up to 76 days following the first VRC01v23 infusion (black arrows/dotted lines = anti-CD20 infusions, blue arrows/dashed lines = VRC01v23 infusions).

(B) Pharmacokinetics (PK) of VRC01v23 (blue, solid shapes) represented by plasma concentration of the bNAb (LOD = 0.3 µg/mL) for up to 76 days following the first bNAb infusion. Plasma viral loads (red, hollow shapes) of each animal respectively shown for evaluation of VRC01v23 effect on viremia. Each point in the PK curves represent the mean of at least two replicates and the error bar represents the standard error. See also Figure S3.

Table 1. Half-life of VRC01v23 in rhesus macaques after different 10 mg/kg dosing regimens

SHIV-infected animal	After first 3 doses (Days)	After 4th and 5th doses (Days)
NHP 1	27.6	27.1
NHP 2	12.1	
NHP 3	13.0	15.1
NHP 4	24.6	
NHP 5	16.4	
SHIV-naïve animal*	After 1 dose (Days)	
NHP A	19.2	
NHP B	13.7	
NHP C	12.2	

*bNAb half-life determined prior to point of rapid plasma clearance for animals with ADA.

through nearly 10 weeks following the last bNAb infusion until VRC01v23 was very low in the plasma at around 8 μg/mL (2B, top middle, Figure S3). NHP 4 had viremia drop below the limit of detection prior to bNAb infusion, suggesting natural control of the virus. This suppression was maintained through the entire study, preventing assessment of bNAb virologic effect in this animal (2B, bottom left).

Absence of ADA responses against VRC01v23

Plasma samples from these VRC01v23-infused animals were tested by ELISA for binding to the VRC01v23 antibody to detect ADA responses. In a parallel pharmacokinetic (PK) study which gave naive rhesus macaques a single 10 mg/kg IV infusion of VRC01v23, 2 out of 3 animals quickly developed significant ADA responses (Figure 3A). The endpoint titer of macaque plasma binding to the bNAb steadily increased over the first 5–6 weeks in these 2 animals (NHP B and C), corresponding to a substantial drop in PK of the bNAb once titers reached a threshold of around 10,000. NHP A showed a steadily increasing endpoint titer but did not appear to reach this threshold at which PK is substantially affected within the first few weeks following bNAb infusion. These ADA responses were observed after a single infusion of VRC01v23 and occurred within just a few weeks of the infusion. When assessed for specificity of binding, these responses showed higher titers against the whole IgG rather than the Fab, suggesting the Fc region was predominantly targeted (Figure S4). By contrast, the 5 animals of this study which underwent B cell depletion prior to VRC01v23 infusion received three 10 mg/kg doses of the bNAb with minimal development of ADA endpoint titers (Figure 3B). These titers displayed some fluctuation by week, but did not reach the threshold of significance established in the earlier trial for ADA with a functional effect on PK. The PK curves of the bNAb in these 5 animals closely resemble the slow and steady decrease of bNAb plasma concentration seen initially in NHP A from the earlier study, suggesting no effect of the ADA response on PK following B cell depletion.

Reinfusions with VRC01v23 following viral rebound

We proceeded with two additional infusions of VRC01v23 into NHPs 1 and 3 that still had B cells depleted at day 68 to assess if rebound virus was still VRC01v23-sensitive (Figures 4A and 4B). The plasma VRC01v23 levels after these additional infusions showed no significant difference in half-lives from those after the first set of infusions ($p = 0.65$) with a gradual decline in antibody levels over time, indicative of an absence of ADA response (Table 1 and Figure 4C). This was further confirmed directly by an ADA ELISA in which endpoint titers did not exceed 1,000 (Figure 4C). At the time of reinfusion, B cells were still depleted and began to return in these animals within 2–4 weeks of the 4th VRC01v23 infusion. Even with the return of B cells, these animals still showed no significant development of ADA response against VRC01v23. Although VRC01v23 levels were high in the plasma following reinfusion, there was minimal to no effect of the bNAb infusion on plasma viremia. NHP 1 showed only a 1 $\log_{10}$ reduction in viremia, and in NHP 3, viremia was not noticeably altered from its post-rebound baseline. This minimal change contrasts with the potent 3–4 $\log_{10}$ reduction in viremia seen in these animals following the first set of VRC01v23 infusions, suggesting that the post-rebound viral quasispecies may be resistant to VRC01v23.

DISCUSSION

The SHIV-infected NHP model serves as an effective *in vivo* model of HIV infection and treatment regimens. Infusion with human bNAbs in NHPs, however, results in the development of ADA responses that prevent

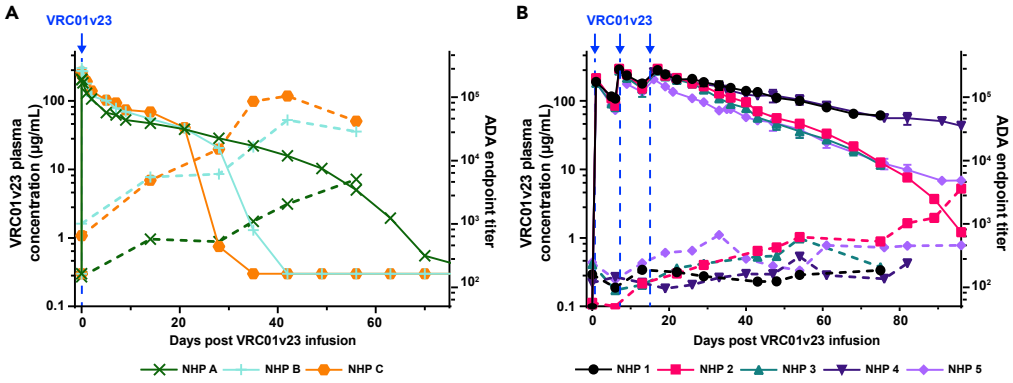

Figure 3. Anti-drug antibody responses against VRC01v23 infusions and effect on pharmacokinetics

(A) Plasma anti-drug antibody ELISA endpoint titers against the bNAb VRC01v23 (ADA, dashed lines) and bNAb pharmacokinetics (PK, solid lines) after one 10 mg/kg IV infusion (blue arrow) in naive animals which did not receive anti-CD20 (control).

(B) ADA endpoint titers (dashed lines, LOD = 50) and VRC01v23 PK (solid lines) after three 10 mg/kg IV infusions (blue arrows) in SHIV-infected animals which received anti-CD20 (treatment). Each point in the PK curves represent the mean of at least two replicates and the error bar represents the standard error. See also Figure S4.

multiple infusions and study of bNAb efficacy over longer periods of time. In this study, the depletion of $CD20^+$ B cells in SHIV-infected rhesus macaques prior to treatment with three 10 mg/kg infusions of the bNAb VRC01v23 inhibited the development of an ADA response. None of the 5 animals with depleted B cells developed a significant ADA response for as long as B cells were depleted. Whereas, in a parallel study evaluating PK of this bNAb in naive macaques, anti-bNAb endpoint titers for all 3 animals increased over time following a single 10 mg/kg infusion. Two animals developed higher ADA responses that correlated with a significant and sharp decrease in bNAb plasma concentration after only 4–5 weeks following infusion once anti-bNAb titers reached approximately 10,000.

The infusions with the anti-CD20 antibody resulted in a rapid drop in B cell levels in all animals following the first infusion. B cells remained depleted in these animals for an average of 13 weeks, beginning to recover as early as 8 weeks or as late as 18 weeks following the final anti-CD20 treatment. This depletion lasted much longer than that shown in another study with the same dosing regimen of rituximab, in which rhesus macaques began recovering B cells within 2–4 weeks of the last infusion (Carroll et al., 2011). The longer term depletion observed in our animals may be related to their chronically SHIV-infected status, as chronic infection without treatment will compromise the immune system. The afucosylation of our anti-CD20 antibody improves antibody-dependent cellular cytotoxicity (Chung et al., 2012) and the rhesusization likely improves half-life over that of unmodified rituximab. These modifications in combination may have resulted in a more complete and longer lasting depletion of $CD20^+$ B cells. Other studies have depleted $CD20^+$ B cells in NHPs using treatment with rituximab, the antibody from which this anti-CD20 was derived, or obinutuzumab, a newer generation of anti-CD20 antibody (Freeman and Sehn, 2018; Grimm et al., 2019). In one study characterizing the PK and B cell depletion of obinutuzumab in cynomolgus macaques, strong ADA responses against the anti-CD20 infusion were seen in 3 out of 4 animals resulting in loss of obinutuzumab in plasma as early as 9 days following infusion (Grimm et al., 2019). This rapid decline of the anti-CD20 antibody corresponded with an increase in B cells once the antibody reached low or undetectable levels. The use of a rhesusized anti-CD20 antibody in our study avoids possible ADA responses associated with infusion of a chimeric humanized antibody into rhesus macaques, allowing for swift and sustained depletion of B cells following multiple infusions of anti-CD20. In past studies involving $CD20^+$ B cell depletion and SIV or SHIV infection, the investigative focus has been on the effect of *de novo* humoral responses on viremia (Gaufin et al., 2009; Miller et al., 2007; Schmitz et al., 2003; Tasca et al., 2011). This study is the first to use $CD20^+$ B cell depletion in chronically SHIV-infected macaques. Here, the pre-existing anti-Env titers dropped slightly following depletion, but remained at relatively high levels that returned to baseline corresponding with the recovery of $CD20^+$ B cells. Total IgG levels fluctuated in all animals prior to the study and were slightly reduced following depletion, but similarly returned to around the baseline with B cell recovery. This is similar to what was observed in one study of rhesus macaques that underwent $CD20^+$ B cell depletion prior to challenge with human influenza A, 4–8 months after an initial challenge with the same viral stock (Carroll et al., 2011). Hemagglutination inhibition titers remained high and even increased after challenge despite B cells being depleted, suggesting that humoral responses are not

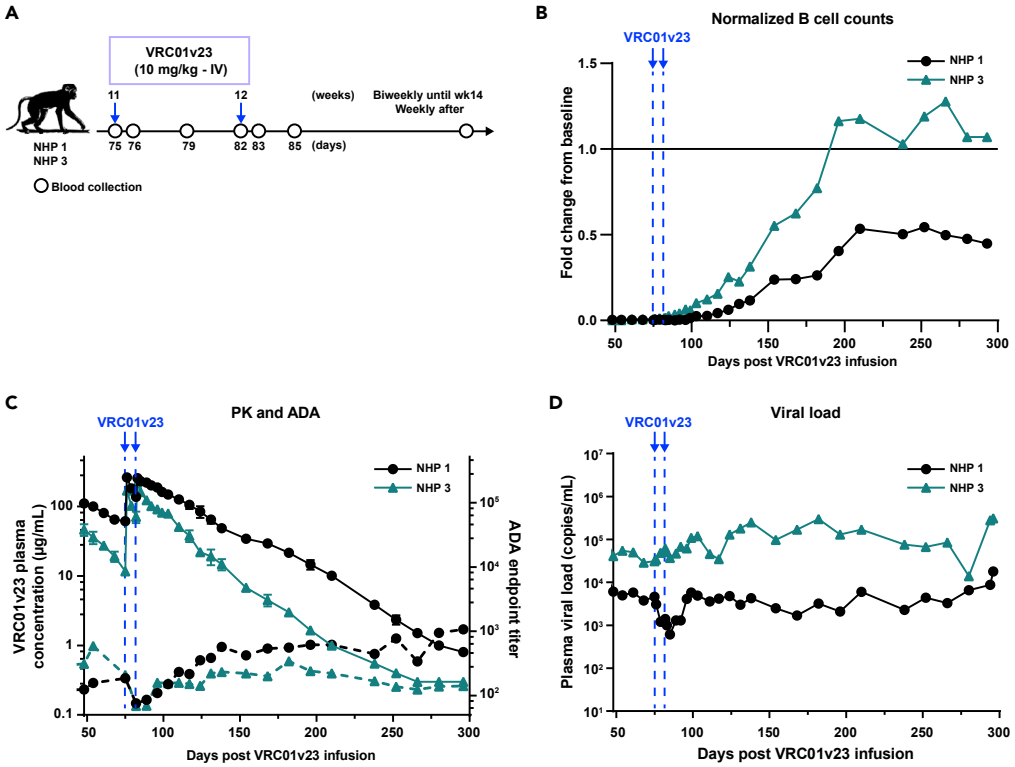

Figure 4. Reinfusions with VRC01v23 following viral rebound

(A) IV infusion schedule of study animals that still had B cells depleted when viremia had rebounded and stabilized. Two weekly infusions of 10 mg/kg bNAb VRC01v23 (blue arrows) given 62 days after the last bNAb infusion from the original treatment schedule. Blood was sampled at indicated timepoints over the course of the study.

(B) B cell counts in whole blood obtained by flow cytometry for each macaque normalized to its B cell count average of day −37 and day −30 of bNAb infusion, prior to CD20 depletion (blue arrows/dashed lines = VRC01v23 infusions).

(C) VRC01v23 PK (solid lines) and ADA endpoint titers (dashed lines) after the two 10 mg/kg IV reinfusions. Each point in the PK curves represent the mean of at least two replicates and the error bar represents the standard error.

(D) Plasma viral load baseline levels after initial rebound and response to reinfusion of VRC01v23.

compromised by $CD20^+$ B cell depletion. This may be due to the relatively long half-life of IgG in sera, as well as the survival of $CD20^-$ plasmablasts following CD20 depletion as seen in humans treated with rituximab (Leandro, 2013). Maintenance of plasmablasts and plasma cells would allow for pre-existing humoral responses to remain during depletion of $CD20^+$ B cells while novel responses are prevented. Finally, although anti-CD20 treatment is an accepted clinical intervention for certain immune disorders, the treatment regimen proposed in this study is intended for improvement of preclinical models only. The generation of ADA responses to bNAbs mainly occurs in animal models since infusion with human bNAbs will be more immunogenic in animals than in humans (Lee et al., 2021). While ADA can occur when protein therapeutics are given in the clinic (Song et al., 2016), $CD20^+$ B cell depletion would be a drastic measure for addressing this problem where the risk of immunosuppression would outweigh any potential benefit to the administered therapy. This study serves to improve the preclinical modeling of bNAbs such that they can be better evaluated prior to attempting translation into a clinical setting.

The pharmacokinetic profile of VRC01v23 after infusion varied between animals in this study. The animals split into two distinct groups where the half-life was determined to be either 12–16 days or 24–27 days. This degree of variation is not normally seen in animal studies of infusions with a single antibody when using naive animals, except in cases where ADA responses drastically reduce half-life. In this case, both of these groups display a slow and steady decline in plasma concentrations of VRC01v23 unaffected by ADA, so these distinct PK profiles are likely due to animal-to-animal variation or a function of their chronic SHIV infection. The ongoing viral replication in these animals may enable VRC01v23 to bind to either HIV Env on virions or on the surface of infected cells in these animals and thereby have an impact on its PK profile depending on the extent of this binding for each animal. Overall, we were able to assess the PK profile of VRC01v23 in these animals and its impact on viremia after infusion

without any ADA responses. There was a 2–4 log_{10} reduction observed in all viremic animals suggesting a strong anti-viral effect of VRC01v23 infusion and confirming the potent anti-viral activity of this bNAb. Other studies with bNAbs in similar SHIV-NHP models show more modest reductions of 1–1.5 log_{10}, further highlighting the increased potency of VRC01v23 compared to those bNAbs (Asokan et al., 2020; Bolton et al., 2015; Julg et al., 2017). In addition, the viral rebound observed in some of the animals during the period of declining levels of VRC01v23 suggest selection of VRC01v23-resistant variants which has been observed in both animal studies and clinical trials using single bNAb treatment regimens (Caskey et al., 2015, 2017; Julg et al., 2017; Lynch et al., 2015; Scheid et al., 2016; Stephenson et al., 2021). Therefore, to minimize the potential for viral escape, treatment regimens with combinations of bNAbs or use of multispecific bNAbs will be needed for HIV infections (Pegu et al., 2022; Wagh et al., 2016).

Infusion of xenogeneic human antibodies or antibody-like proteins into nonhuman primates often leads to ADA responses that neutralize the functional activity of these antibodies by binding and rapidly clearing them from circulation (Bolton et al., 2015; Lee et al., 2021; Pegu et al., 2015; Rosenberg et al., 2019; Shapiro et al., 2020). This limits the number of infusions that can be performed with such human proteins and hampers the evaluation of the long-term effects of these treatments in the SHIV-NHP model. In naive animals infused with VRC01v23, significant ADA responses primarily against the human Fc region of the bNAb developed within 4 weeks of infusion and prevented accurate measurement of its pharmacokinetic properties. This ADA response differs from what would be seen in a clinical setting where occasional ADA responses occur but do not target the Fc region. The mitigation of ADA by B cell depletion in the current study provides a strategy to evaluate human antibody-based therapies in the SHIV-NHP model. The use of B cell depletion to minimize immune responses has been successfully tested in xenotransplantation models in rhesus macaques, demonstrating the potential of this approach to mitigate generation of *de novo* immune responses against transplanted tissues (Choi et al., 2018; Kim et al., 2018). In those studies, there was no initial immune response to the transplanted tissue during the B cell depletion phase, but there was eventually an immune response to the transplant once the B cells returned. This suggests there is only a transient impairment in the generation of *de novo* humoral responses which is achieved during periods of B cell depletion. In the current study, the B cell depletion resulted in loss of B cells from circulation for up to 5 months from the first anti-CD20 infusion and enabled us to deliver two additional VRC01v23 infusions without any ADA generation in two animals. Although B cells returned in these two animals shortly after the 4^{th} and 5^{th} infusions with VRC01v23, no ADA responses developed. This suggests a prolonged period in which we can assess the efficacy of human bNAb-based immunotherapies in the SHIV-NHP model without the appearance of ADA. Additionally, multiple rounds of anti-CD20 infusions can help maintain B cell depletion, further extending the period of such evaluation. This can facilitate the preclinical assessment of novel immunotherapies that require prolonged treatment regimens such as use of antibodies together with latency reversal agents to treat or cure HIV (Dashti et al., 2020; Pegu et al., 2015; Pincus et al., 2021; Sloan et al., 2015; Sung et al., 2015; Tuyishime et al., 2021; Tuyishime and Ferrari, 2020). Furthermore, use of prolonged treatment with bNAb-based immunotherapies can help us to evaluate the development of viral escape variants in the SHIV-NHP model and to assess the pathways for viral escape, as well as to select more promising therapies that limit such escape *in vivo* for further clinical evaluation.

Limitations of the study

A limitation of this study was the small sample size of 5 animals. Therefore, this was a pilot study with very promising results that will need to be expanded upon using a larger cohort of animals in future studies. Due to limited animal availability, no control group of SHIV-infected animals that received bNAbs without B cell depletion was included. Since many published studies have already documented ADA following infusions of bNAbs in SHIV-infected animals (Bolton et al., 2015; Lee et al., 2021; Rosenberg et al., 2019; Shapiro et al., 2020), we proceeded without such a control group. Additionally, there are some potential limitations to the use of B cell depletion that should be explored in future studies. We do not know whether any synergistic effects between infused bNAbs and B cells may have altered the efficacy of our bNAb against the SHIV infection. There may also have been some immunosuppressive effect of B cell depletion impacting anti-viral T cell immune responses in these animals, which need to be investigated in more detail in follow-up studies. Lastly, there are potential concerns for the overall health of the animals throughout the depletion regimen; however, several studies have looked at longer term B cell depletion in humans as a rheumatoid arthritis treatment and saw no ill health effects (Isvy et al., 2012; van Vollenhoven et al., 2015; Winthrop et al., 2018).

In conclusion, these data suggest that B cell depletion can prevent the development of ADA responses and improve the evaluation of bNAb therapies in a SHIV-infected rhesus macaque model, making this a promising strategy for use in future preclinical trials that more closely resemble clinical treatment regimens.

STAR★METHODS

Detailed methods are provided in the online version of this paper and include the following:

- KEY RESOURCES TABLE
- RESOURCE AVAILABILITY
  - Lead contact
  - Materials availability
  - Data and code availability
- EXPERIMENTAL MODEL AND SUBJECT DETAILS
  - Animal study design
- METHOD DETAILS
  - Generation of monoclonal antibodies
  - Plasma viral load quantification
  - Flow cytometric analysis of blood cell counts
  - ELISA to measure plasma concentration of antibody infusions
  - ELISA to measure anti-drug antibody responses
  - ELISA to endogenous SHIV-directed humoral responses
  - ELISA to measure total monkey IgG levels
- QUANTIFICATION AND STATISTICAL ANALYSIS

SUPPLEMENTAL INFORMATION

Supplemental information can be found online at https://doi.org/10.1016/j.isci.2022.105067.

ACKNOWLEDGMENTS

We thank Alida Taylor, Saran Bao, and Jumugal Noor from the VRC Translational Research Program for animal research support, and Brenda Hartman for assistance with graphics. The anti-CD20 [2B8R1F8]-Afucosylated antibody used in this study was provided by the NIH Nonhuman Primate Reagent Resource (P40 OD028116). Support for this work was provided by the Intramural Research Program of the Vaccine Research Center, National Institute of Allergy and Infectious Diseases, NIH.

AUTHOR CONTRIBUTIONS

S.E.L. and A.P. initiated, led, and designed the NHP study and performed the analyses; S.E.L., S.H.H., R.A.K., J.R.M., and A.P. prepared figures and co-wrote the manuscript; S.E.L. and S.H.H. processed all NHP samples and performed flow cytometric analysis of these samples; S.E.L., E.S.Y., and M.L.F. performed PK and ADA ELISAs; C.L., M.C., and X.C. provided reagents for ELISAs; E.M., J-P.T., and R.A.W. coordinated the NHP study; J.R.M. and A.P. headed the study and co-wrote the manuscript with all authors providing comments and revisions.

DECLARATION OF INTERESTS

The authors declare no competing interests.

Received: May 9, 2022
Revised: July 21, 2022
Accepted: August 30, 2022
Published: October 21, 2022

REFERENCES

Asokan, M., Dias, J., Liu, C., Maximova, A., Ernste, K., Pegu, A., McKee, K., Shi, W., Chen, X., Almasri, C., et al. (2020). Fc-mediated effector function contributes to the in vivo antiviral effect of an HIV neutralizing antibody. Proc. Natl. Acad. Sci. USA *117*, 18754–18763.

Bar-On, Y., Gruell, H., Schoofs, T., Pai, J.A., Nogueira, L., Butler, A.L., Millard, K., Lehmann, C., Suarez, I., Oliveira, T.Y., et al. (2018). Safety and antiviral activity of combination HIV-1 broadly neutralizing antibodies in viremic individuals. Nat. Med. *24*, 1701–1707.

Barouch, D.H., Whitney, J.B., Moldt, B., Klein, F., Oliveira, T.Y., Liu, J., Stephenson, K.E., Chang, H.W., Shekhar, K., Gupta, S., et al. (2013). Therapeutic efficacy of potent neutralizing HIV-1-specific monoclonal antibodies in SHIV-infected rhesus monkeys. Nature *503*, 224–228.

Bauer, A.M., and Bar, K.J. (2020). Advances in simian–human immunodeficiency viruses for nonhuman primate studies of HIV prevention and cure. Curr. Opin. HIV AIDS *15*, 275–281.

Bolton, D.L., Pegu, A., Wang, K., McGinnis, K., Nason, M., Foulds, K., Letukas, V., Schmidt, S.D., Chen, X., Todd, J.P., et al. (2015). Human immunodeficiency virus type 1 monoclonal antibodies suppress acute simian-human immunodeficiency virus viremia and limit seeding

of cell-associated viral reservoirs. J. Virol. *90*, 1321–1332.

Carroll, T.D., Matzinger, S.R., Fritts, L., McChesney, M.B., and Miller, C.J. (2011). Memory B cells and CD8(+) lymphocytes do not control seasonal influenza A virus replication after homologous re-challenge of rhesus macaques. PLoS One *6*, e21756.

Caskey, M., Klein, F., Lorenzi, J.C.C., Seaman, M.S., West, A.P., Jr., Buckley, N., Kremer, G., Nogueira, L., Braunschweig, M., Scheid, J.F., et al. (2015). Viraemia suppressed in HIV-1-infected humans by broadly neutralizing antibody 3BNC117. Nature *522*, 487–491.

Caskey, M., Schoofs, T., Gruell, H., Settler, A., Karagounis, T., Kreider, E.F., Murrell, B., Pfeifer, N., Nogueira, L., Oliveira, T.Y., et al. (2017). Antibody 10-1074 suppresses viremia in HIV-1-infected individuals. Nat. Med. *23*, 185–191.

Choi, S.H., Yoon, C.H., Lee, H.J., Kim, H.P., Kim, J.M., Che, J.H., Roh, K.M., Choi, H.J., Kim, J., Hwang, E.S., et al. (2018). Long-term safety outcome of systemic immunosuppression in pig-to-nonhuman primate corneal xenotransplantation. Xenotransplantation *25*, e12442.

Chung, S., Quarmby, V., Gao, X., Ying, Y., Lin, L., Reed, C., Fong, C., Lau, W., Qiu, Z.J., Shen, A., et al. (2012). Quantitative evaluation of fucose reducing effects in a humanized antibody on Fcgamma receptor binding and antibody-dependent cell-mediated cytotoxicity activities. mAbs *4*, 326–340.

Cohen, Y.Z., Butler, A.L., Millard, K., Witmer-Pack, M., Levin, R., Unson-O'Brien, C., Patel, R., Shimeliovich, I., Lorenzi, J.C.C., Horowitz, J., et al. (2019). Safety, pharmacokinetics, and immunogenicity of the combination of the broadly neutralizing anti-HIV-1 antibodies 3BNC117 and 10-1074 in healthy adults: a randomized, phase 1 study. PLoS One *14*, e0219142.

Corey, L., Gilbert, P.B., Juraska, M., Montefiori, D.C., Morris, L., Karuna, S.T., Edupuganti, S., Mgodi, N.M., deCamp, A.C., Rudnicki, E., et al. (2021). Two randomized trials of neutralizing antibodies to prevent HIV-1 acquisition. N. Engl. J. Med. *384*, 1003–1014.

Crowell, T.A., Colby, D.J., Pinyakorn, S., Sacdalan, C., Pagliuzza, A., Intasan, J., Benjapornpong, K., Tangnaree, K., Chomchey, N., Kroon, E., et al. (2019). Safety and efficacy of VRC01 broadly neutralising antibodies in adults with acutely treated HIV (RV397): a phase 2, randomised, double-blind, placebo-controlled trial. Lancet. HIV *6*, e297–e306.

Crowley, A.R., Osei-Owusu, N.Y., Dekkers, G., Gao, W., Wuhrer, M., Magnani, D.M., Reimann, K.A., Pincus, S.H., Vidarsson, G., and Ackerman, M.E. (2021). Biophysical evaluation of rhesus macaque Fc gamma receptors reveals similar IgG Fc glycoform preferences to human receptors. Front. Immunol. *12*, 754710.

Dashti, A., Waller, C., Mavigner, M., Schoof, N., Bar, K.J., Shaw, G.M., Vanderford, T.H., Liang, S., Lifson, J.D., Dunham, R.M., et al. (2020). SMAC mimetic plus triple-combination bispecific HIVxCD3 retargeting molecules in SHIV.C.CH505-infected, antiretroviral therapy-suppressed rhesus macaques. J. Virol. *94*, e00793-20.

Edupuganti, S., Mgodi, N., Karuna, S.T., Andrew, P., Rudnicki, E., Kochar, N., deCamp, A., De La Grecca, R., Anderson, M., Karg, C., et al. (2021). Feasibility and successful enrollment in a proof-of-concept HIV prevention trial of VRC01, a broadly neutralizing HIV-1 monoclonal antibody. J. Acquir. Immune Defic. Syndr. *87*, 671–679.

Freeman, C.L., and Sehn, L.H. (2018). A tale of two antibodies: obinutuzumab versus rituximab. Br. J. Haematol. *182*, 29–45.

Gaudinski, M.R., Coates, E.E., Houser, K.V., Chen, G.L., Yamshchikov, G., Saunders, J.G., Holman, L.A., Gordon, I., Plummer, S., Hendel, C.S., et al. (2018). Safety and pharmacokinetics of the Fc-modified HIV-1 human monoclonal antibody VRC01LS: a Phase 1 open-label clinical trial in healthy adults. PLoS Med. *15*, e1002493.

Gaudinski, M.R., Houser, K.V., Doria-Rose, N.A., Chen, G.L., Rothwell, R.S.S., Berkowitz, N., Costner, P., Holman, L.A., Gordon, I.J., Hendel, C.S., et al. (2019). Safety and pharmacokinetics of broadly neutralising human monoclonal antibody VRC07-523LS in healthy adults: a phase 1 dose-escalation clinical trial. Lancet. HIV *6*, e667–e679.

Gaufin, T., Gautam, R., Kasheta, M., Ribeiro, R., Ribka, E., Barnes, M., Pattison, M., Tatum, C., MacFarland, J., Montefiori, D., et al. (2009). Limited ability of humoral immune responses in control of viremia during infection with SIVsmmD215 strain. Blood *113*, 4250–4261.

Griffith, S.A., and McCoy, L.E. (2021). To bnAb or not to bnAb: defining broadly neutralising antibodies against HIV-1. Front. Immunol. *12*, 708227.

Grimm, H.P., Schick, E., Hainzl, D., Justies, N., Yu, L., Klein, C., Husar, E., and Richter, W.F. (2019). PKPD assessment of the anti-CD20 antibody obinutuzumab in cynomolgus monkey is feasible despite marked anti-drug antibody response in this species. J. Pharm. Sci. *108*, 3729–3736.

Isvy, A., Meunier, M., Gobeaux-Chenevier, C., Maury, E., Wipff, J., Job-Deslandre, C., Kahan, A., and Allanore, Y. (2012). Safety of rituximab in rheumatoid arthritis: a long-term prospective single-center study of gammaglobulin concentrations and infections. Joint Bone Spine *79*, 365–369.

Julg, B., Pegu, A., Abbink, P., Liu, J., Brinkman, A., Molloy, K., Mojta, S., Chandrashekar, A., Callow, K., Wang, K., et al. (2017). Virological control by the CD4-binding site antibody N6 in simian-human immunodeficiency virus-infected rhesus monkeys. J. Virol. *91*, e00498-17.

Kim, J., Choi, S.H., Lee, H.J., Kim, H.P., Kang, H.J., Kim, J.M., Hwang, E.S., Park, C.G., and Kim, M.K. (2018). Comparative efficacy of anti-CD40 antibody-mediated costimulation blockade on long-term survival of full-thickness porcine corneal grafts in nonhuman primates. Am. J. Transplant. *18*, 2330–2341.

Klein, C., Jamois, C., and Nielsen, T. (2021). Anti-CD20 treatment for B-cell malignancies: current status and future directions. Expert Opin. Biol. Ther. *21*, 161–181.

Kwon, Y.D., Asokan, M., Gorman, J., Zhang, B., Liu, Q., Louder, M.K., Lin, B.C., McKee, K., Pegu, A., Verardi, R., et al. (2021). A matrix of structure-based designs yields improved VRC01-class antibodies for HIV-1 therapy and prevention. mAbs *13*, 1946918.

Kwon, Y.D., Pancera, M., Acharya, P., Georgiev, I.S., Crooks, E.T., Gorman, J., Joyce, M.G., Guttman, M., Ma, X., Narpala, S., et al. (2015). Crystal structure, conformational fixation and entry-related interactions of mature ligand-free HIV-1 Env. Nat. Struct. Mol. Biol. *22*, 522–531.

Leandro, M.J. (2013). B-cell subpopulations in humans and their differential susceptibility to depletion with anti-CD20 monoclonal antibodies. Arthritis Res. Ther. *15*, S3.

Lee, W.S., Reynaldi, A., Amarasena, T., Davenport, M.P., Parsons, M.S., and Kent, S.J. (2021). Anti-drug antibodies in pigtailed macaques receiving HIV broadly neutralising antibody PGT121. Front. Immunol. *12*, 749891.

Li, H., Wang, S., Lee, F.H., Roark, R.S., Murphy, A.I., Smith, J., Zhao, C., Rando, J., Chohan, N., Ding, Y., et al. (2021). New SHIVs and improved design strategy for modeling HIV-1 transmission, immunopathogenesis, prevention and cure. J. Virol. *95*. JVI.00071-21.

Lynch, R.M., Boritz, E., Coates, E.E., DeZure, A., Madden, P., Costner, P., Enama, M.E., Plummer, S., Holman, L., Hendel, C.S., et al. (2015). Virologic effects of broadly neutralizing antibody VRC01 administration during chronic HIV-1 infection. Sci. Transl. Med. *7*. 319ra206.

Mahomed, S., Garrett, N., Karim, Q.A., Zuma, N.Y., Capparelli, E., Baxter, C., Gengiah, T., Archary, D., Samsunder, N., Rose, N.D., et al. (2020). Assessing the safety and pharmacokinetics of the anti-HIV monoclonal antibody CAP256V2LS alone and in combination with VRC07-523LS and PGT121 in South African women: study protocol for the first-in-human CAPRISA 012B phase I clinical trial. BMJ Open *10*, e042247.

Maloney, D.G., Grillo-López, A.J., White, C.A., Bodkin, D., Schilder, R.J., Neidhart, J.A., Janakiraman, N., Foon, K.A., Liles, T.M., Dallaire, B.K., et al. (1997). IDEC-C2B8 (Rituximab) anti-CD20 monoclonal antibody therapy in patients with relapsed low-grade non-Hodgkin's lymphoma. Blood *90*, 2188–2195.

Marshall, M.J.E., Stopforth, R.J., and Cragg, M.S. (2017). Therapeutic antibodies: what have we learnt from targeting CD20 and where are we going? Front. Immunol. *8*, 1245.

Mayer, K.H., Seaton, K.E., Huang, Y., Grunenberg, N., Isaacs, A., Allen, M., Ledgerwood, J.E., Frank, I., Sobieszczyk, M.E., Baden, L.R., et al. (2017). Safety, pharmacokinetics, and immunological activities of multiple intravenous or subcutaneous doses of an anti-HIV monoclonal antibody, VRC01, administered to HIV-uninfected adults: results of a phase 1 randomized trial. PLoS Med. *14*, e1002435.

McFarland, E.J., Cunningham, C.K., Muresan, P., Capparelli, E.V., Perlowski, C., Morgan, P., Smith, B., Hazra, R., Purdue, L., Harding, P.A., et al. (2021). Safety, tolerability, and pharmacokinetics of a long-acting broadly neutralizing human immunodeficiency virus type 1 (HIV-1)

monoclonal antibody VRC01LS in HIV-1-Exposed newborn infants. J. Infect. Dis. *224*, 1916–1924.

McLaughlin, P., Grillo-López, A.J., Link, B.K., Levy, R., Czuczman, M.S., Williams, M.E., Heyman, M.R., Bence-Bruckler, I., White, C.A., Cabanillas, F., et al. (1998). Rituximab chimeric anti-CD20 monoclonal antibody therapy for relapsed indolent lymphoma: half of patients respond to a four-dose treatment program. J. Clin. Oncol. *16*, 2825–2833.

Mendoza, P., Gruell, H., Nogueira, L., Pai, J.A., Butler, A.L., Millard, K., Lehmann, C., Suárez, I., Oliveira, T.Y., Lorenzi, J.C.C., et al. (2018). Combination therapy with anti-HIV-1 antibodies maintains viral suppression. Nature *561*, 479–484.

Miller, C.J., Genescà, M., Abel, K., Montefiori, D., Forthal, D., Bost, K., Li, J., Favre, D., and McCune, J.M. (2007). Antiviral antibodies are necessary for control of simian immunodeficiency virus replication. J. Virol. *81*, 5024–5035.

Nishimura, Y., Donau, O.K., Dias, J., Ferrando-Martinez, S., Jesteadt, E., Sadjadpour, R., Gautam, R., Buckler-White, A., Geleziunas, R., Koup, R.A., et al. (2021). Immunotherapy during the acute SHIV infection of macaques confers long-term suppression of viremia. J. Exp. Med. *218*, e20201214.

Pegu, A., Asokan, M., Wu, L., Wang, K., Hataye, J., Casazza, J.P., Guo, X., Shi, W., Georgiev, I., Zhou, T., et al. (2015). Activation and lysis of human CD4 cells latently infected with HIV-1. Nat. Commun. *6*, 8447.

Pegu, A., Xu, L., DeMouth, M.E., Fabozzi, G., March, K., Almasri, C.G., Cully, M.D., Wang, K., Yang, E.S., Dias, J., et al. (2022). Potent anti-viral activity of a trispecific HIV neutralizing antibody in SHIV-infected monkeys. Cell Rep. *38*, 110199.

Permar, S.R., Klumpp, S.A., Mansfield, K.G., Carville, A.A.L., Gorgone, D.A., Lifton, M.A., Schmitz, J.E., Reimann, K.A., Polack, F.P., Griffin, D.E., and Letvin, N.L. (2004). Limited contribution of humoral immunity to the clearance of measles viremia in rhesus monkeys. J. Infect. Dis. *190*, 998–1005.

Pincus, S.H., Craig, R.B., Weachter, L., LaBranche, C.C., Nabi, R., Watt, C., Raymond, M., Peters, T., Song, K., Maresh, G.A., et al. (2021). Bispecific anti-HIV immunoadhesins that bind Gp120 and Gp41 have broad and potent HIV-neutralizing activity. Vaccines *9*, 774.

Qin, M., Wang, L., Wu, D., Williams, C.K., Xu, D., Kranz, E., Guo, Q., Guan, J., Vinters, H.V., Lee, Y., et al. (2019). Enhanced delivery of rituximab into brain and lymph nodes using timed-release nanocapsules in non-human primates. Front. Immunol. *10*, 3132.

Rosenberg, Y.J., Lewis, G.K., Montefiori, D.C., LaBranche, C.C., Lewis, M.G., Urban, L.A., Lees, J.P., Mao, L., and Jiang, X. (2019). Introduction of the YTE mutation into the non-immunogenic HIV bnAb PGT121 induces anti-drug antibodies in macaques. PLoS One *14*, e0212649.

Scheid, J.F., Horwitz, J.A., Bar-On, Y., Kreider, E.F., Lu, C.L., Lorenzi, J.C.C., Feldmann, A., Braunschweig, M., Nogueira, L., Oliveira, T., et al. (2016). HIV-1 antibody 3BNC117 suppresses viral rebound in humans during treatment interruption. Nature *535*, 556–560.

Schmitz, J.E., Kuroda, M.J., Santra, S., Simon, M.A., Lifton, M.A., Lin, W., Khunkhun, R., Piatak, M., Lifson, J.D., Grosschupff, G., et al. (2003). Effect of humoral immune responses on controlling viremia during primary infection of rhesus monkeys with simian immunodeficiency virus. J. Virol. *77*, 2165–2173.

Schommers, P., Gruell, H., Abernathy, M.E., Tran, M.K., Dingens, A.S., Gristick, H.B., Barnes, C.O., Schoofs, T., Schlotz, M., Vanshylla, K., et al. (2020). Restriction of HIV-1 escape by a highly broad and potent neutralizing antibody. Cell *180*, 471–489.e22.

Shapiro, M.B., Cheever, T., Malherbe, D.C., Pandey, S., Reed, J., Yang, E.S., Wang, K., Pegu, A., Chen, X., Siess, D., et al. (2020). Single-dose bNAb cocktail or abbreviated ART post-exposure regimens achieve tight SHIV control without adaptive immunity. Nat. Commun. *11*, 70.

Shingai, M., Nishimura, Y., Klein, F., Mouquet, H., Donau, O.K., Plishka, R., Buckler-White, A., Seaman, M., Piatak, M., Jr., Lifson, J.D., et al. (2013). Antibody-mediated immunotherapy of macaques chronically infected with SHIV suppresses viraemia. Nature *503*, 277–280.

Sloan, D.D., Lam, C.Y.K., Irrinki, A., Liu, L., Tsai, A., Pace, C.S., Kaur, J., Murry, J.P., Balakrishnan, M., Moore, P.A., et al. (2015). Targeting HIV reservoir in infected CD4 T cells by dual-affinity Re-targeting molecules (DARTs) that bind HIV envelope and recruit cytotoxic T cells. PLoS Pathog. *11*, e1005233.

Sok, D., and Burton, D.R. (2018). Recent progress in broadly neutralizing antibodies to HIV. Nat. Immunol. *19*, 1179–1188.

Song, S., Yang, L., Trepicchio, W.L., and Wyant, T. (2016). Understanding the supersensitive anti-drug antibody assay: unexpected high anti-drug antibody incidence and its clinical relevance. J. Immunol. Res. *2016*, 3072586.

Spencer, D.A., Goldberg, B.S., Pandey, S., Ordonez, T., Dufloo, J., Barnette, P., Sutton, W.F., Henderson, H., Agnor, R., Gao, L., et al. (2022). Phagocytosis by an HIV antibody is associated with reduced viremia irrespective of enhanced complement lysis. Nat. Commun. *13*, 662.

Stephenson, K.E., Julg, B., Tan, C.S., Zash, R., Walsh, S.R., Rolle, C.P., Monczor, A.N., Lupo, S., Gelderblom, H.C., Ansel, J.L., et al. (2021). Safety, pharmacokinetics and antiviral activity of PGT121, a broadly neutralizing monoclonal antibody against HIV-1: a randomized, placebo-controlled, phase 1 clinical trial. Nat. Med. *27*, 1718–1724.

Sung, J.A.M., Pickeral, J., Liu, L., Stanfield-Oakley, S.A., Lam, C.Y.K., Garrido, C., Pollara, J., LaBranche, C., Bonsignori, M., Moody, M.A., et al. (2015). Dual-Affinity Re-Targeting proteins direct T cell-mediated cytolysis of latently HIV-infected cells. J. Clin. Invest. *125*, 4077–4090.

Tasca, S., Zhuang, K., Gettie, A., Knight, H., Blanchard, J., Westmoreland, S., and Cheng-Mayer, C. (2011). Effect of B-cell depletion on coreceptor switching in R5 simian-human immunodeficiency virus infection of rhesus macaques. J. Virol. *85*, 3086–3094.

Tuyishime, M., Dashti, A., Faircloth, K., Jha, S., Nordstrom, J.L., Haynes, B.F., Silvestri, G., Chahroudi, A., Margolis, D.M., and Ferrari, G. (2021). Elimination of SHIV infected cells by combinations of bispecific HIVxCD3 DART® molecules. Front. Immunol. *12*, 710273.

Tuyishime, M., and Ferrari, G. (2020). Engineering antibody-based molecules for HIV treatment and cure. Curr. Opin. HIV AIDS *15*, 290–299.

van Vollenhoven, R.F., Fleischmann, R.M., Furst, D.E., Lacey, S., and Lehane, P.B. (2015). Longterm safety of rituximab: final report of the rheumatoid arthritis global clinical trial program over 11 years. J. Rheumatol. *42*, 1761–1766.

Wagh, K., Bhattacharya, T., Williamson, C., Robles, A., Bayne, M., Garrity, J., Rist, M., Rademeyer, C., Yoon, H., Lapedes, A., et al. (2016). Optimal combinations of broadly neutralizing antibodies for prevention and treatment of HIV-1 clade C infection. PLoS Pathog. *12*, e1005520.

Walsh, S.R., and Seaman, M.S. (2021). Broadly neutralizing antibodies for HIV-1 prevention. Front. Immunol. *12*, 712122.

Wen, J., Cheever, T., Wang, L., Wu, D., Reed, J., Mascola, J., Chen, X., Liu, C., Pegu, A., Sacha, J.B., et al. (2021). Improved delivery of broadly neutralizing antibodies by nanocapsules suppresses SHIV infection in the CNS of infant rhesus macaques. PLoS Pathog. *17*, e1009738.

Winthrop, K.L., Saag, K., Cascino, M.D., Pei, J., John, A., Jahreis, A., Haselkorn, T., and Furst, D.E. (2018). Long-term safety of rituximab in rheumatoid arthritis: analysis from the SUNSTONE registry. Arthritis Care Res. *71*, 993–1003.

Yoon, C.H., Choi, S.H., Choi, H.J., Lee, H.J., Kang, H.J., Kim, J.M., Park, C.G., Choi, K., Kim, H., Ahn, C., and Kim, M.K. (2020). Long-term survival of full-thickness corneal xenografts from alpha1, 3-galactosyltransferase gene-knockout miniature pigs in non-human primates. Xenotransplantation *27*, e12559.

STAR★METHODS

KEY RESOURCES TABLE

REAGENT or RESOURCE	SOURCE	IDENTIFIER
Antibodies		
VRC01v23	This paper	N/A
Anti-CD20 [2B8R1F8]-Afucosylated	NIH Nonhuman Primate Reagent Resource Program	AB_2819341
Chemicals, peptides, and recombinant proteins		
VRC01v23 anti-idiotype Ab	This paper	N/A
Cynomolgus CD20/MS4A1 Full Length Protein, His Tag	Acro Biosystems	CD0-C52H8
biotinylated BG505 DS-SOSIP HIV-1 env trimer	(Kwon et al., 2015)	N/A
Critical commercial assays		
Monkey IgG ELISA Kit	Immunology Consultants Laboratory	E-85G
Experimental models: Organisms/strains		
Indian origin rhesus macaque	This paper	N/A
Software and algorithms		
GraphPad Prism Software	GraphPad Prism Software, Inc.	SCR_002798
FlowJo software	BD biosciences	SCR_008520

RESOURCE AVAILABILITY

Lead contact

Further information and requests for resources and reagents should be directed to and will be fulfilled by Amarendra Pegu (pegua@niaid.nih.gov).

Materials availability

All new reagents are available by MTA for non-commercial research.

Data and code availability

- All data reported in this paper will be shared by the lead contact upon request.
- This paper does not report original code.
- Any additional information required to reanalyze the data reported in this paper is available from the lead contact upon request.

EXPERIMENTAL MODEL AND SUBJECT DETAILS

Animal study design

All animals (5 male and 2 female rhesus macaques, aged 4–7 years) were housed and cared for in an AAALAC International accredited facility at the National Institutes of Health (NIH) and in accordance with policies outlined in the USDA Animal Welfare Act, the Public Health Services Policy on Human Care and Use of Laboratory Animals and the *Guide for Care and Use of Laboratory Animals*. All animal procedures and experiments were performed according to a research protocol approved by the Institutional Animal Care and Use Committee of the National Institute of Allergy and Infectious Diseases (NIAID). These animals previously participated in an IACUC approved SHIV challenge research study, in which naive rhesus macaques were intrarectally challenged with $SHIV_{BG505}$. In brief, animals were inoculated intrarectally with one milliliter of a 1:8 dilution of challenge stock. This corresponds to an animal infectious dose of approximately 5 based on the reported AID_{50} titer which was 1 mL of 1:120 dilution of the challenge stock (Li et al., 2021). The animals were infected for a period of 1–4 years and then used in this study. They were administered an afucosylated rhesusized anti-CD20 antibody (Crowley et al., 2021) (<1 EU/mg) intravenously at 50 mg of Ab/kilogram of body weight (mg/kg) on days -30, -16, and -2. These animals were then infused

with 3 doses of VRC01v23 at 10 mg/kg on days 0, 6, and 13. Two animals were reinfused later with VRC01v23 at the same dose on days 75 and 82.

METHOD DETAILS

Generation of monoclonal antibodies

VRC01v23 was either produced from a stably transfected CHO cell line or from transiently transfected Expi293 cells and purified by protein A column. The rituximab-based afucosylated rhesusized anti-CD20 antibody was obtained from the National Institutes of Health Nonhuman Primate Reagent Resource Program.

Plasma viral load quantification

Plasma viremia was quantitated using a PCR-based method to quantify SIV gag RNA levels with a detection limit of 15 copies/milliliter as described previously (Bolton et al., 2015).

Flow cytometric analysis of blood cell counts

Whole blood samples were collected throughout the study and stained with a panel of fluorochrome-conjugated antibodies specific for various leukocyte surface markers which were titrated for optimal binding. The rituximab-based afucosylated rhesusized anti-CD20 antibody used in this study can block binding of the anti-CD20 conjugate used for detection of B cells, so an anti-CD19 conjugate was included for verification of B cell depletion. Counts were taken of $CD20^+$ and/or $CD19^+$ B cells, $CD3^+CD4^+$ T cells, and $CD3^+CD8^+$ T cells within the leukocyte population at each collection. Rhesus macaque-reactive antibody conjugates used were: anti-NHP CD45-FITC (BD biosciences Cat#552566, RRID: AB_394433, clone D058-1283), anti-human CD16-BUV496 (BD biosciences, Cat#612944, RRID: AB_2870224, clone 3G8), anti-human CD3-APC-Cy7 (BD biosciences, Cat#557757, RRID: AB_396863, clone SP34-2), anti-CD8a-PE (Beckman Coulter, Cat#IM0452U, RRID: AB_131202, clone B9.11), anti-CD19-PE-Cy5 (Beckman Coulter, Cat#IM2643U, RRID: AB_131160, clone J3-119), anti-CD20-PacBlue (Biolegend, Cat#302328, RRID: AB_1595435, clone 2H7), anti-CD4-AF700 clone (Biolegend, Cat#317426, RRID: AB_571943, OKT4), anti-CD14-BV510 (Biolegend, Cat#301842, RRID: AB_2561946, clone M5E2), and anti-HLA-DR-PE- Cy5.5 (Thermo Fisher, Cat#MHLDR18, RRID: AB_10372966, clone TU36). The antibody panel was added to the bottom of a Trucount Absolute Counting Tube (BD Biosciences) and 150 μL of whole blood was then added and left to incubate for 15 min. 1350 mL were then added of a 1X preparation of BD FACS Lysing Solution (BD Biosciences) in sterile water. After at least 30 min, samples were loaded onto a 96-well round bottom plate for HTS acquisition on an LSRFortessa X50 flow cytometer (BD Biosciences). Data were concatenated by sample and analyzed using FlowJo v10 software (BD Biosciences).

For the anti-CD20 competition assay, frozen PBMCs were thawed, washed with 1xPBS and 2×10^6 cells were incubated with 10, 5, 2.5, 1.25, 0.63 μg or no afucosylated rhesusized anti-CD20 antibody on ice for 30 min. Cells were washed twice with 1xPBS and treated with antibody cocktail containing the surface antibodies described above. For PBMC staining anti-CD14-BV510 was replaced with the LIVE/DEAD Fixable Aqua Dead Cell dye (Thermofisher), which was added to the cells after addition of the surface staining antibody cocktail without washing. Surface staining was conducted on ice for 30 min and cells were washed twice with 1xPBS. Cells were resuspended in 200 μL of 1% PFA solution and acquired on an LSRFortessa X50 flow cytometer (BD Biosciences). Data were analyzed using FlowJo v10 software (BD Biosciences).

For the B cell depletion verification by CD19 staining, frozen PBMCs were thawed, washed with 1xPBS and 2×10^6 cells were incubated with antibody cocktail containing the surface antibodies described above. Anti-CD14-BV510 was replaced with the LIVE/DEAD Fixable Aqua Dead Cell dye (Thermofisher), which was added to the cells after addition of the surface staining antibody cocktail without washing. Cells were incubated with antibody cocktail for 30 min, followed by two washes with 1xPBS. Cells were resuspended in 200 μL of 1% PFA solution and acquired on an LSRFortessa X50 flow cytometer (BD Biosciences). Data were analyzed using FlowJo v10 software (BD Biosciences).

ELISA to measure plasma concentration of antibody infusions

VRC01v23 levels were measured using quantitative ELISA-based methods (limit of detection = 0.3 μg/mL) in which microtiter plates coated overnight at 4°C with 2 μg/mL anti-idiotype antibody in PBS were used to

capture the administered antibodies followed by detection using a horseradish peroxidase (HRP)-conjugated anti-human IgG antibody (Jackson Immunoresearch). After coating, microtiter plates were washed with PBS-T (PBS with 0.05% Tween 20) and blocked with TBS containing 5% skim milk, 2% BSA and 0.1% Tween 20 (blocking buffer). Plasma from macaques was diluted in blocking buffer. Diluted samples were incubated on the plates alongside standard curves of known antibody concentration for 1 h at room temperature followed by a PBS-T wash. The plates were then incubated with a 1:10,000 dilution of HRP-conjugated anti-human IgG antibody in blocking buffer for 30 min at room temperature. The plates were washed with PBS-T, then SureBlue TMB (Kirkegaard & Perry Laboratories, Gaithersburg, MD) substrate was added. The plates were allowed to develop for 15 min in the dark, then stopped with 1N H_2SO_4 before reading the optical density at 450 nm. Afucosylated rhesusized anti-CD20 levels were similarly measured using His-tagged cynomolgus CD20 (Acro Biosystems) on Nickel-coated plates (Thermo Fisher) followed by detection with an HRP-conjugated anti-monkey IgG, Fc-specific (Southern Biotech) with a limit of detection of 31 μg/mL.

ELISA to measure anti-drug antibody responses

Plasma from macaques was diluted with TBS containing 5% skim milk, 2% BSA and 0.1% Tween 20 (blocking buffer). 5-fold serial dilutions ranging from 1:50 to 1:781,250 of these plasmas were then added in duplicate wells to 96-well microtiter plates that had been coated overnight at 4°C with 2 μg/mL of VRC01v23 and blocked with blocking buffer. The plates were incubated for 1 h at room temperature followed by a PBS-T (PBS with 0.05% Tween 20) wash. Bound monkey IgGs were then probed with a 1:8,000 dilution of HRP-conjugated anti-monkey IgG, Fc-specific (Southern Biotech) in blocking buffer for 30 min at room temperature. The plates were then washed, and SureBlue TMB (Kirkegaard & Perry Laboratories, Gaithersburg, MD) substrate was added. Once color developed (typically 15 to 20 min), stopping buffer (1N H_2SO_4) was added and the optical density at 450 nm was read. Endpoint titers were calculated by determining the lowest dilution that had an optical density greater than 5-fold of that in the background wells incubated with only blocking buffer instead of a plasma dilution.

ELISA to endogenous SHIV-directed humoral responses

ELISAs were conducted as specified under measurement of anti-drug antibody responses. Streptavidin-coated plates were coated overnight at 4°C with biotinylated BG505 HIV Env trimer and bound antibodies were probed with HRP-conjugated anti-monkey IgG, Fc-specific (Southern Biotech).

ELISA to measure total monkey IgG levels

The Monkey IgG ELISA kit from Immunology Consultants Laboratory, Inc. was used for evaluation of IgG levels in macaque plasma over time. Kit protocols were followed, and heat-inactivated plasma used in prior ELISAs was diluted at the recommended 1:80,000 for detection of a value within the range of the standard curve.

QUANTIFICATION AND STATISTICAL ANALYSIS

Statistical analysis comparing half-lives of VRC01v23 in reinfused animals between first and second rounds of infusions was performed using a two-tailed paired samples t-test.